

Electrical and thermal transport properties of the alloy system $(\text{Ce}_{1-x}\text{La}_x)\text{Cu}_4\text{In}$

Aiman K Bashir¹, Moise B Tchoula Tchokonté¹, Douglas Britz², B M Sondezi³, André M Strydom² Dariusz Kaczorowski³

¹Department of Physics, University of the Western Cape, Private Bag X 17, Bellville 7535, South Africa

²Highly Correlated Matter Research Group, Department of Physics, University of Johannesburg, PO Box 524, Auckland Park 2006, South Africa

³Institute of Low Temperature and Structure Research, Polish Academy of Sciences, PO Box 1410, 50 - 950 Wrocław, Poland

E-mail: mtchokonte@uwc.ac.za (M B Tchoula Tchokonté)

Abstract. The studies of electrical resistivity, $\rho(T)$, magnetoresistivity, MR, thermoelectric power, $S(T)$ and thermal conductivity, $\lambda(T)$, of the alloy system $(\text{Ce}_{1-x}\text{La}_x)\text{Cu}_4\text{In}$ ($0 \leq x \leq 1$) are reported. The room temperature powder X-ray diffraction studies confirm the orthorhombic $\text{CeCu}_{4.38}\text{In}_{1.62}$ - type crystal structure with space group $Pnmm$ (No. 58) for all investigated compositions across the series. $\rho(T)$ results indicate an evolution from coherent Kondo scattering to incoherent single - ion Kondo scattering, with increased La content x . $\rho(T)$ for each composition at high temperature is described by a $-\ln(T)$ behaviour. MR measurements on Ce dilute alloys are interpreted within the single - ion Bethe ansatz description of the Coqblin - Schrieffer model. $S(T)$ results are described by the phenomenological resonance model. $\lambda(T)$ data increase linearly with temperature from low T and shows a tendency toward saturation above 300 K for dilute Ce alloys. The Lorentz number, L/L_0 and the dimensionless figure of merit, $ZT = S^2T/\lambda\rho$ increase upon cooling and exhibit maxima at low temperatures.

1. Introduction

CeCu_5 is well known to be an antiferromagnetic (AF) Kondo lattice compound with $T_N = 4$ K [1]. The substitutions of one Cu with elements of the p - block (M), increase the average conduction electron density, which screen the localized $4f$ moments state in CeCu_5 leading to a non magnetic heavy -Fermion (HF) ground state in CeCu_4M [2, 3, 4]. Several experimental investigations were reported on the series CeCu_4M , (M = Al, Ga, In) [2, 3, 4, 5, 6]. Transport, magnetic and thermodynamic properties studies of the CeCu_4M compounds have confirmed the HF state with an electronic specific heat coefficient taking huge values of the order of 2 - 3 $\text{J.K}^{-2}.\text{mol}^{-1}$. The transport properties studies indicate a Kondo temperature in the range 2 - 5 K from the $\rho(T)$ measurement [3, 5, 6], while the thermoelectric power shows positive values with large peak at a temperature in the range 20 - 30 K [4, 6].

The studies of magnetic and electronic properties of CeCu_4In compound in particular [6, 7], indicate paramagnetic behaviour down to 2 K that follows the Curie - Weiss law with effective magnetic moment $2.40 \mu_B$ and paramagnetic Weiss temperature $\theta_p = -27$ K. Heat capacity studies confirm the HF character for this compound with the electronic heat capacity coefficient



$\gamma = 235 \text{ mJ/mole.K}^2$. $\rho(T)$ behaviour is characteristic of a Kondo lattice compound with a well defined resistivity maximum at 25 K.

In the current paper, we report on the study of the electrical and thermal transport properties of the alloy system $(\text{Ce}_{1-x}\text{La}_x)\text{Cu}_4\text{In}$.

2. Results and discussion

2.1. Lattice parameters and unit - cell volume

The crystal structure was checked and confirmed by the powder X-ray diffraction technique, using the $\text{CuK}\alpha$ radiation ($\lambda = 1.5406 \text{ \AA}$). We have observed that all the compositions crystallize in the orthorhombic $Pnmm$ system [No. 58] [9]. The lattice parameters and the unit cell volume obtained for the CeCu_4In are in good agreement with previously reported values [6]. It is observed that the refined room - temperature lattice parameters a , b and c and the unit - cell volume V increase linearly with increased La content x (see figure 1). The observed linear increase in V confirms the Vegard's rule which suggests no sudden change in the Ce valence across the series.

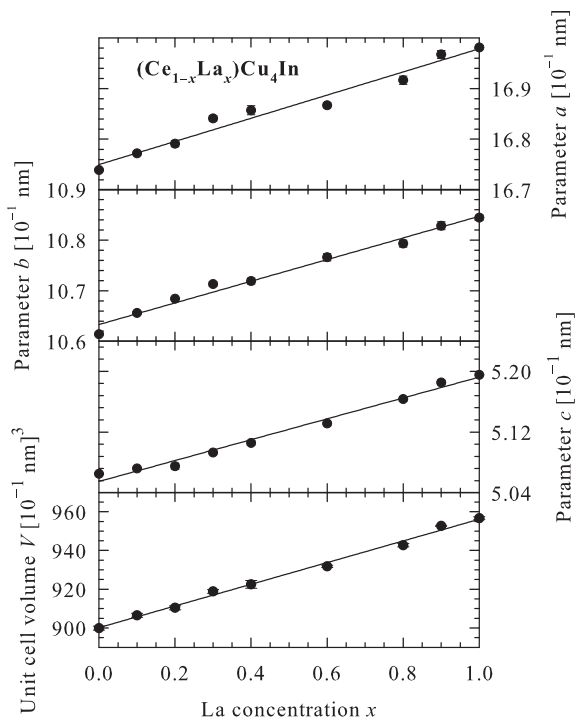


Figure 1. Lattice parameters a , b and c and unit cell volume V as a function of La content x of $(\text{Ce}_{1-x}\text{La}_x)\text{Cu}_4\text{In}$.

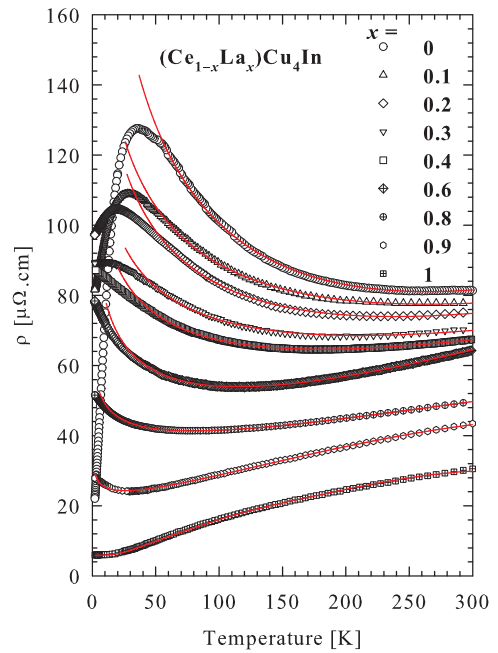


Figure 2. (color online) $\rho(T)$ for the $(\text{Ce}_{1-x}\text{La}_x)\text{Cu}_4\text{In}$ alloy system. The solid red lines are LSQ fits of Eqs.1 and 2 to the measured data.

2.2. Electrical transport

2.2.1. Electrical resistivity: The temperature dependence of the zero - field total resistivity $\rho(T)$ of alloys in the series $(\text{Ce}_{1-x}\text{La}_x)\text{Cu}_4\text{In}$ is shown in figure 2. It is observed that $\rho(T)$ evolves from coherent Kondo behaviour at low temperatures for alloys in the range $0 \leq x \leq 0.3$,

with a well defined Kondo peak at T_{max}^{ρ} as indicated in table 1 to incoherent single - ion Kondo behaviour for alloys with $x \geq 0.4$. It is observed that T_{max}^{ρ} which is a fair indication of the Kondo temperature T_K for dense Kondo alloys systems, shifts to lower temperature with increased La content x . At higher temperatures for all Ce containing alloys in the series, $\rho(T)$ follows a $-\ln(T)$ as is to be expected for incoherent Kondo scattering. $\rho(T)$ of the non - magnetic counterpart LaCu₄In departs from linearity at high temperatures and is described by the Bloch - Grüneisen - Mott formula:

$$\rho(T) = \rho_0 + \frac{4\kappa}{\theta_R} \cdot \left(\frac{T}{\theta_R}\right)^5 \int_0^{\theta_R/T} \frac{x^5 dx}{(e^x - 1)(1 - e^{-x})} - \alpha T^3, \quad (1)$$

where all the parameters have their usual meaning. Least - squares (LSQ) fit of Eq.(1) to the experimental $\rho(T)$ for the LaCu₄In (solid line in figure 2) gives $\rho_0 = 5.95 \mu\Omega.cm$, $\kappa = 2000 \mu\Omega.cm.K$, $\theta_R = 132$ K and $\alpha = 0.31 \times 10^{-8} \mu\Omega.cm.K^{-3}$. $\rho(T)$ curves for all compositions where incoherent Kondo scattering is observed are described by

$$\rho(T) = \rho_0' + \rho_{ph}(T) - C_K \ln(T), \quad (2)$$

where ρ_0' is the residual resistivity. It is observed that LSQ fits of $\rho(T)$ data to Eq. 2 for alloys with $x \leq 0.6$, the interband scattering that seems to be present for alloys with $x \geq 0.8$ is suppressed with 40% Ce doping. For this reason we include only the second term in $\rho_{ph}(T)$ in Eq.(1) and approximate it to $\rho_{ph}(T) = bT$ for compositions with $x \leq 0.8$. The Mott's term ($-\alpha T^3$) was included only for alloys with $x = 0.8$ and 0.9 . LSQ fits of Eq.(2) to $\rho(T)$ data (solid lines figure 2) yield $\rho(T)$ parameters listed in table 1 and $\alpha[10^{-8} \mu\Omega.cm/K^3] = 4.3(3)$ and $23(2)$ for the $x = 0.8$ and 0.9 alloys respectively.

2.2.2. Magnetoresistivity: The isothermal MR was studied on a selected number of (Ce_{1-x}La_x)Cu₄In alloys for which their $\rho(T)$ curves are characteristic of incoherent Kondo scattering. The results of these studies are presented in figure 3 for two representative compositions $x = 0.6$ and 0.8 . As shown in figure 3 for the investigated alloys, a negative MR has been observed at all temperatures as a result of suppression of the incoherent Kondo scattering in magnetic field. We proceed to analyze the results in terms of the Bethe - ansatz calculation of the Coqblin - Schrieffer model given by Andrei [11] and Schlottmann [12] for total angular momentum $J = 1/2$ in the integer valence limit

$$\frac{\rho(B, T)}{\rho(B = 0, T)} = \left[\frac{1}{2J + 1} \sin^2\left(\frac{\pi n_f}{2J + 1}\right) \sum_{\ell=0}^{2J} \sin^{-2}(\pi n_{\ell}) \right]^{-1}, \quad (3)$$

where n_f is the electron occupation number. The solid lines in the main panel of figure 3 show fits of the experimental isothermal MR data according to Eq. 3 and this yields values of the characteristic Kondo field B^* which is related to the Kondo temperature T_K according to the relation [13]

$$B^*(T) = B^*(0) + \frac{k_B T}{g\mu_K} = \frac{k_B(T_K^{MR} + T)}{g\mu_K}, \quad (4)$$

where the parameters have their usual meaning. LSQ fits of Eq. 4 to these B^* values obtained at the isotherms in the main panel of figure 3 are represented by solid lines in the inset of figure 3 and the obtained values of T_K^{MR} and μ_K are listed in table 1. The values of μ_K decrease with increase in La content. Similarly to T_{max}^{ρ} , it is also observed that T_K^{MR} values decrease monotonically with increase in La content, which results from the increase in unit - cell volume which in turn weakens the on - site Kondo exchange interaction according to the compressible Kondo lattice model [14]. Similar behaviour of T_K^{MR} and μ_K was observed in many diluted Ce alloys [10]. Finally, figure 4 illustrates the excellent scaling of the MR data in accordance with the Bethe ansatz formulation of the single - ion MR by showing the collapse of MR data from all isotherms on a single curve.

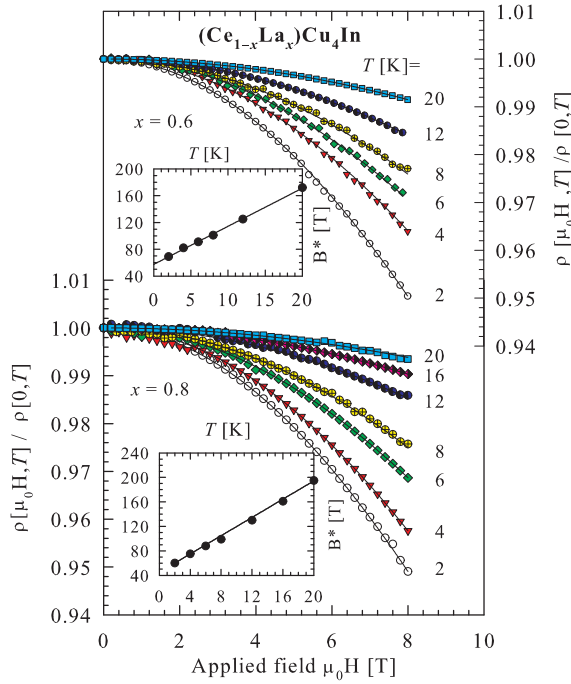


Figure 3. (color online) MR isotherms at various temperature. The solid lines in the main panel are LSQ fits of Eq. 3 to the measured data. The insets shows the temperature variation of $B^*(T)$, and the solid lines through the data points are an LSQ fit of Eq. 4 to the B^* values.

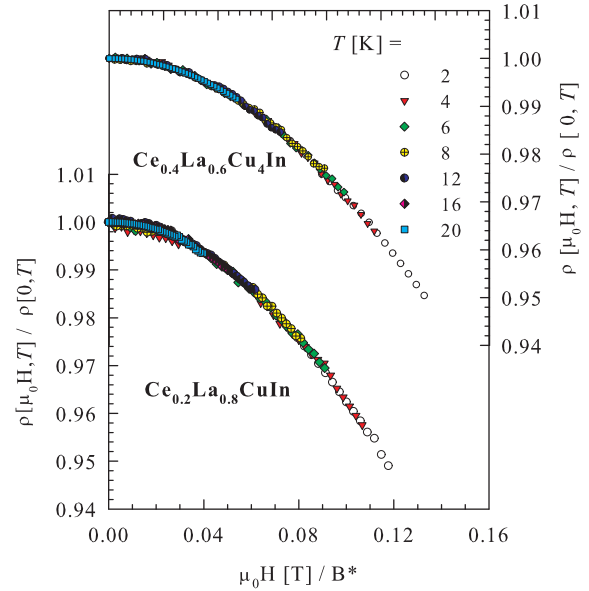


Figure 4. (color online) Scaling of MR data for different isotherms as measured in field up to 8 T and at various temperatures between 2 and 20 K.

Table 1. Electrical and thermal transport data for the $(\text{Ce}_{1-x}\text{La}_x)\text{Cu}_4\text{In}$ alloy system. These values are obtained from LSQ fits of Eqs. 1, 2, 3 4 and 5 to the measured data (see text).

x	0	0.1	0.2	0.3	0.4	0.6	0.8	0.9
$\rho_0[\mu\Omega.\text{cm}]$	336(4)	227(3)	216(2)	158(1)	139.7(2)	115.4(2)	63.2(2)	31.1(1)
$b[10^{-3}\mu\Omega.\text{cm}/\text{K}]$	210(8)	124(7)	133(3)	98(3)	99(4)	142(3)	82(7)	118(2)
$C_K[\mu\Omega.\text{cm}]$	56(1)	33(1)	31.7(5)	20.5(4)	17.9(1)	16.4(1)	6.5(1)	3.03(4)
$T_{max}^\rho[\text{K}]$	34.0(1)	27.9(1)	17.8(1)	13.4(1)				
$T_K^{MR}[\text{K}]$				20.1(3)	11.3(8)	10.1(2)	6.0(4)	
$\mu_K[\mu_B]$				0.412(8)	0.340(3)	0.305(5)	0.233(1)	
$T_K^S[\text{K}]$	21.8(7)	17.3(6)				14.9(7)	10.7(4)	
$a[\mu\text{V}/\text{K}^2]$	0.022(2)	0.029(4)				0.024(5)	0.018(3)	
$T_{CEF}[\text{K}]$	95(2)	94(2)				98(3)	96(2)	

2.3. Thermal transport

2.3.1. Thermoelectric power: The combined results of the TEP of selected compositions in the alloys series $(\text{Ce}_{1-x}\text{La}_x)\text{Cu}_4\text{In}$ are shown in figure 5A. The results obtained are typical of heavy

- fermion compounds characterized by one peak below room temperature and differ drastically to that of a normal metal [4]. For all investigated compositions, $S(T)$ is positive in the whole temperature range and exhibit a maximum roughly at the same temperature of 30 K. The observed $S(T)$ maximum decreases in magnitude with increased La content x . We have carried out the analysis of the measured $S(T)$ data in terms of the phenomenological resonance model [15], which describes the low temperature $S(T)$ data. This model assumes that the dominant contribution to $S(T)$ originates from the scattering of electrons from a wide conduction band into a narrow f - band approximated by a Lorentzian shape. According to the model, two parameters must be taken into account: the position of the f - electron band relative to Fermi level ($E_f - E_F$) and the width of the resonance peak W_f . Thus, the temperature variation of $S(T)$ can then be expressed in the form

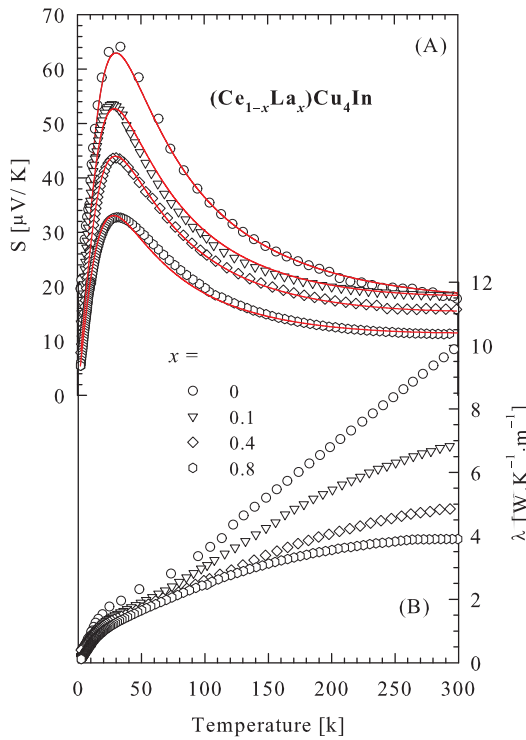


Figure 5. (color online) Temperature dependence (A) of $S(T)$ and (B) $\lambda(T)$. The solid lines in the panel (A) are LSQ fits of Eq.5 to the measured data.

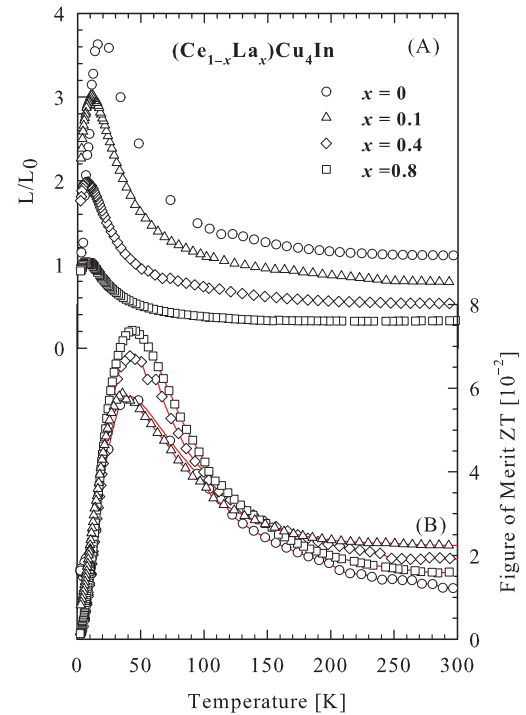


Figure 6. (color online) Temperature dependence (A) of the Lorentz number L/L_0 and (B) the Figure of merits ZT .

$$S(T) = \frac{2 k_B}{3 |e|} \frac{\pi^2 T E_f}{(\pi^2/3) T^2 + E_f^2 + W_f^2} + S_d(T), \quad (5)$$

where $S_d(T) = aT$ is the Mott's contribution originating from the interband scattering, E_f and W_f have the unit of temperature (K). The first term in Eq.5 describes very well $S(T)$ of mixed valence system due to their high value of T_K . Therefore, to obtain a good fit shown by solid line in figure 5A we have included the Mott's term and made a similar assumption as in Ref.[7] taking $E_f = T_K^S$ and $W_f = \pi T_{CEF}/N_f$, where N_f is the orbital degeneracy $2J + 1$ and T_{CEF} the characteristic temperature which is a measure of the CEF. LSQ fits of Eq.5 to the experimental

$S(T)$ data give the parameters listed in table 1. The behaviour of T_K^S with La content is similar to that of T_{max}^ρ and T_K^{MR} . The resulting parameters obtained for our parent compound CeCu₄In are in good agreement with previously reported results [7].

2.3.2. Thermal conductivity: Figure 5B shows the results of $\lambda(T)$ of selected compositions in the alloys series (Ce_{1-x}La_x)Cu₄In. The thermal conductivity of metals originates from two contributions: an electron component $\lambda_e(T)$ and a lattice component $\lambda_{ph}(T)$ for which phonons are heat carriers. It is observed that the slope of the linear part of $\lambda(T)$ in the temperature range $50K \leq T \leq 150K$, is increased with decreasing La content x . At temperatures below 20 K, $\lambda(T)$ is proportional to T , which is typical for scattering of electrons on lattice imperfections. At temperatures above 150 K, $\lambda(T)$ for diluted Ce alloys deviate from linearity, with a downward curvature and a tendency toward saturation above 300 K. Such a saturation of $\lambda(T)$ follows the Wilson's law which predicts a constant value of $\lambda(T)$, typical for scattering electrons on thermally excited phonons [16]. The linear behaviour of $\lambda(T)$ for the pure Ce compound is not predicted theoretically.

Combining the results of $\lambda(T)$ and $\rho(T)$, we have plotted in figure 6A the Lorentz number $L(T) = \lambda(T)\rho(T)/T$ normalized to the value of $L_0 = 2.45 \times 10^{-8} \text{ W}\cdot\Omega\cdot\text{K}^{-2}$. It is observed that the values of L/L_0 decrease rapidly with increasing La content x . The overall behaviour of L/L_0 for all investigated compositions is a rapid increase on cooling followed by a maximum at a temperature T_{max} which shifts slightly from 16 K to 9 K with increasing in La content x . This is followed by a sudden drop of L/L_0 below T_{max} . The observed maximum decreases in magnitude with increase in La content. The increase of L/L_0 at low temperatures deviates from the Wiedemann - Franz law which predicts $L/L_0 = 1$, and this may be attributed to an additional lattice thermal conductivity or can also arise from the energy dependent Kondo scattering process. Such a tendency was observed for several Ce compounds [7]. Our value of T_{max} observed for our parent compound CeCu₄In is in agreement with the value of 16 K reported in Ref.[7].

Figure 6B presents values of the dimensionless figure of merit $ZT = S^2T/\lambda\rho$, which determines the efficiency of the thermoelectric material. A commonly used thermoelectric material in power generation or refrigeration is Bi₂Te₃ with ZT between 0.8 and 1 [17]. It is observed that ZT values for all the investigated compositions increase on cooling and exhibit a maximum at temperature between 42 and 48 K. The observed peak increases in magnitude with increasing La content, opposite to that of L/L_0 . Our maximum value for CeCu₄In is about 0.06 at $T = 48$ K and ZT takes the value of 12.5×10^{-3} at room temperature. These values are roughly twice larger than the values reported for the same compound in Ref.[18] at $T = 50$ K.

2.4. Conclusions

XRD studies confirm the orthorhombic CeCu_{4.38}In_{1.62} - type crystal structure with space group $Pnmm$. $\rho(T)$ evolves from coherent to incoherent single - ion Kondo scattering. A negative MR and positive $S(T)$ are observed for all investigated compositions. MR data are interpreted within the single - ion Bethe ansatz description of the Coqblin - Schrieffer model. $S(T)$ data are described by the phenomenological resonance model. The resulting values of T_{max}^ρ , T_K^{MR} and T_K^S decrease with increasing La content x which is consistent with the compressible Kondo lattice model. $\lambda(T)$ follows the Wilson's law near 300 K for diluted Ce alloys. L/L_0 and ZT increase rapidly upon cooling followed by a maximum at low temperature.

Acknowledgments

Support is acknowledged from the NRF through grants No.: 81296, 81804 and 91683. AMS thanks the SA-NRF (78832), and the Faculty of Science and URC of UJ for financial assistance.

References

- [1] Bauer E *et al.* 1987 *J. Magn. Magn. Mater.* **69** 158.
- [2] Eichler A *et al.* 1995 *Physica B* **206 - 207** 258.
- [3] Andraka B *et al.* 1991 *Phys. Rev.* **B44** 4371.
- [4] Bauer E *et al.* 1987 *Solid State Commun.* **62** 271.
- [5] Kowalczyk A *et al.* 2009 *J. Phys.: Condens. Matter* **20** 255252.
- [6] Kowalczyk A *et al.* 2009 *J. Alloys Compd.* **481** 40.
- [7] Tolinski T *et al.* 2010 *J. Alloys Compd.* **490** 15.
- [8] Falkowski E *et al.* 1987 *Intermetallics* **19** 433.
- [9] Baraniak M *et al.* 1991 *Izvestiya AN SSSR. Neorgan. Materialy* **27** 1235.
- [10] Tchoula Tchokonte M B *et al.* 2004 *J. Phys.: Condens. Matter* **16** 1981.
- [11] Andrei N 1982 *Phys. Lett. A* **87** 299.
- [12] Schlottmann P 1983 *Z. Phys. B* **51** 223.
- [13] Batlogg B *et al.* 1987 *J. Magn. Magn. Mater.* **63-64** 441.
- [14] Lavagna M *et al.* 1983 *J. Phys. F: Metal Phys.* **13** 1007.
- [15] Gottwich U *et al.* 1985 *J. Magn. Magn. Mater.* **47-48** 536.
- [16] Bauer E *et al.* 1991 *J. Phys.: Condens. Matter* **3** 7641.
- [17] Duck Y C *et al.* 1997 *XVI ICT 97. Proceedings ICT 97* 459.
- [18] Tolinski T *et al.* 2011 *Eur. Phys. J.* **B 84** 177.